Sky view factor as predictor of solar availability on building façades: using the case of London

Christina Chatzipoulka[1, 2], Raphaël Compagnon[1] and Marialena Nikolopoulou[2]

[1] Haute Ecole d'ingénierie et d'architecture de Fribourg (HEIA-FR), Fribourg, Switzerland
[2] Kent School of Architecture, University of Kent, Canterbury, United Kingdom
Correspondence email: chatzipoulka@gmail.com

Abstract: Sky view factor (SVF) measures the openness of a point to the sky vault and as such, has been widely used in urban climatology and environmental design studies associated to various phenomena, including Urban Heat Island intensity and daylight availability. This study examines to what extent SVF can be also employed for predicting solar availability in the urban environment, with emphasis on building façades.

SVF and solar irradiance simulations were performed for vertical façades in 24 urban forms -of 500x500m area- in London; mean values were computed by urban form, and by façade orientation, considering 30 orientations at 12° azimuth intervals. The statistical analysis reveals a strong linear relationship (R^2>0.8) between SVF and annual global irradiance for all orientations. The models derived from linear regression tests were integrated into a graphical tool for predicting annual global irradiance on a façade in London as a function of its SVF and azimuth angle. Furthermore, the fact that SVF was found to correlate well with both major components of solar irradiation, namely direct and sky diffused irradiances, indicates that it can be used for predicting annual solar availability at latitudes similar to London, even for sunnier climates.

Keywords: solar potential, solar indicator, sky view factor, urban façades, orientation

Introduction

Solar energy is one of the renewable energy resources with the greatest potential; it is estimated that, upon certain conditions, solar energy could contribute to 27 per cent of the global electricity production by 2050 (IEA, 2014). Unlike other renewable energy technologies, photovoltaic (PV) systems can be relatively easily applied in the urban environment, integrated into new and existing buildings. A major advantage of exploiting building envelopes for harnessing solar radiation is the on-site production and use of energy which will be a requirement for all new buildings in the European Union after 2020 (EPBD, 2010).

Compared to façades, roofs are regarded more favourable for the implementation of photovoltaic systems as there they are generally less affected by overshadowing and intervene less with buildings' appearance and other functions served by façades (daylighting, natural ventilation, etc.). Nonetheless, with façades comprising the greatest part of urban buildings' surface, their solar irradiation represents a considerable percentage of cities' solar energy potential (Redweik et al., 2013) and hence, their exploitation becomes critical for the attainment of energy efficiency targets at building and urban scale. In response to this challenge, photovoltaics technology is advancing rapidly offering more possibilities for an

improved architectural integration, aesthetically (colours, level of transparency, etc.) and functionally (e.g. providing solar and glare protection).

The potential for integration of PV systems on façades varies significantly in urban areas, as façades' insolation is highly sensitive to urban geometry, affected by orientation and degree of obstruction (Esclapés et al., 2014; Yun and Steemers, 2009). The orientation of an unobstructed façade determines its interaction with the solar geometry at a specific location and thus, its potential solar irradiation. However, urban façades are usually obstructed by surrounding buildings which limits their openness to the sky (related to the sky diffuse solar component) and solar exposure (related to the direct solar component). Past studies, employing statistical analysis, have shown a strong negative relationship between degree of sky obstruction, associated positively to built density, and façades' total solar irradiation (Chatzipoulka et al., 2016; Mohajeri et al., 2016). However, their findings refer to average values over entire urban areas, neglecting the orientation parameter.

This study explores the relationship between the degree of sky obstruction, expressed by sky view factor (SVF), and solar availability on building façades as a function of their orientation. Initially introduced by urban climatologists, sky view factor (SVF) is a measure of the openness of a point to the sky and thus its capability to emit and receive longwave radiation to and from the sky, respectively. In the literature, SVF is equally used as urban geometry variable, e.g. investigating its relationship with spatial variations of urban air and surface temperatures (Eliasson, 1996; Yamashita et al., 1986), and as performance indicator evaluating environmentally different urban forms (Project PREcis, 2000; Ratti et al., 2003). With respect to façades' performance, SVF is widely used as indicator of daylight availability (e.g. Cheng et al., 2006; Zhang et al., 2012), while its relation with solar availability is less established.

In the past, SVF measurements were feasible only in situ and at one point each time, using special equipment such as fish-eye cameras. Nowadays, an increasing number of urban solar and thermal analysis models perform accurate SVF calculations as part of their simulations, over entire urban surfaces and at different spatial resolutions. Compared to solar irradiance simulations, the calculation of SVF is faster and requires solely one input, namely the 3D urban geometry information. In this context, predicting solar availability in urban environments using SVF values would enable a quick evaluation of solar energy potential and facilitate the task of architects and urban designers for integration of efficient solar active strategies in new and existing buildings.

Methodology

Cases studies

This study is part of an on-going research and based on the analysis of twenty-four urban forms, of 500x500m area each, which have been selected from three areas of London. These areas represent urban environments of different built density with the studied urban forms covering values from 3 to 22, m^3/m^2 (total built volume within the site over site area). The results of their geometrical analysis as well as the criteria for their selection are presented analytically in Chatzipoulka et al. (2016). It is noted that the naming of the urban forms as appeared in Figure 1 is reserved for consistency between past and future publications: the letter denotes the area to which an urban form belongs (C, W, N for central, west, north area, respectively), while the number derives from its position in the area's map.
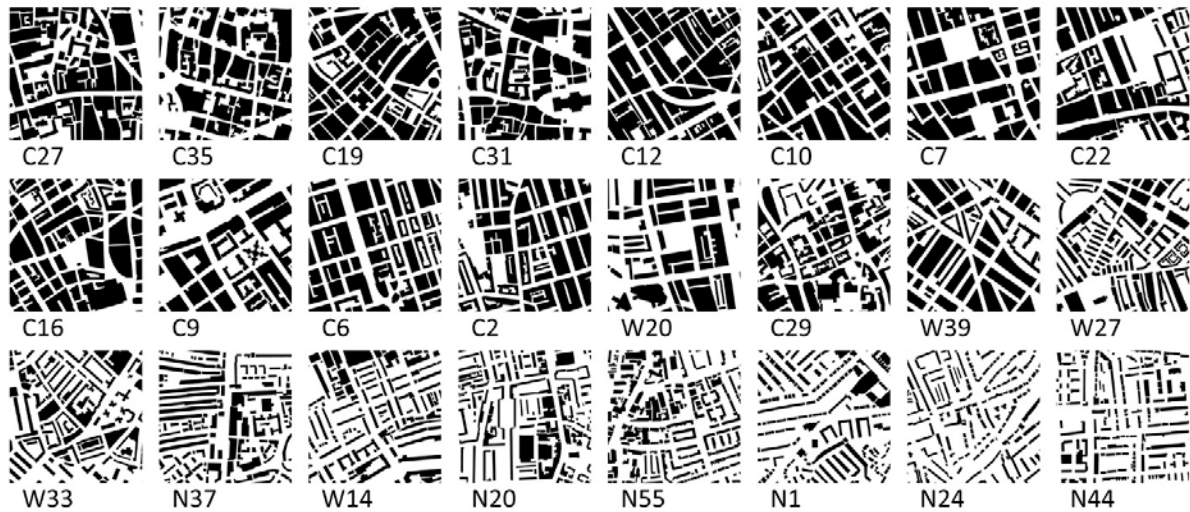
Figure 1. Ground maps of twenty-four urban forms considered in the analysis, in decreasing order of density.

SVF and solar irradiance simulations

Solar simulations have been performed in PPF software, a powerful tool which has been employed by several studies, so far (e.g. Chatzipoulka et al., 2016; Cheng et al., 2006; Project PREcis, 2000). PPF is based on the RADIANCE ray-tracing programme (Ward Larson and Shakespeare, 1998) and uses sky models which represent average radiance distributions of the sky vault for a given time period (Compagnon, 2004). Specifically, for the irradiation simulations, climatic data of London (hourly direct and diffuse irradiance values) were obtained from METEONORM software (Remund et al., 2015) and processed statistically in order to build up London's annual sky model (Fig. 2a). Only daytime hours were considered, i.e. hours between sunrise and sunset on a day, which are 4317 in total. It is worth to be mentioned that, considering the entire year, direct and diffuse horizontal irradiance for London are in a relative balance with the former being 102 and the latter 120, W/m^2.

The 3D digital models of the urban forms were reproduced in a CAD software, including the surrounding buildings, and inserted in PPF (Fig. 2b). Annual mean irradiances [W/m^2] and sky view factor (SVF) [-] values were computed on a grid of 2-meter spatial resolution, adjusted onto the surfaces of the models. Direct (*Id*), diffused from the sky (*Is*) and reflected by buildings (*Ib*) irradiances were computed separately; while global (*Ig*) irradiance is calculated as the sum of them, as described below:

$$Ig = Id + Is + Ib$$

SVF ranges from 0 to 1, denoting a totally obstructed and unobstructed point, respectively; however, façades' SVF value ranges from 0 to 0.5 as unobstructed vertical surfaces can be seen only by half of the sky vault.

The simulation results were processed in Matlab and mean values of four types of irradiances and SVF were computed, first by urban form, and next by orientation in each urban form. The relationships between mean SVF and irradiances were next explored performing linear regression analysis in the same programme.
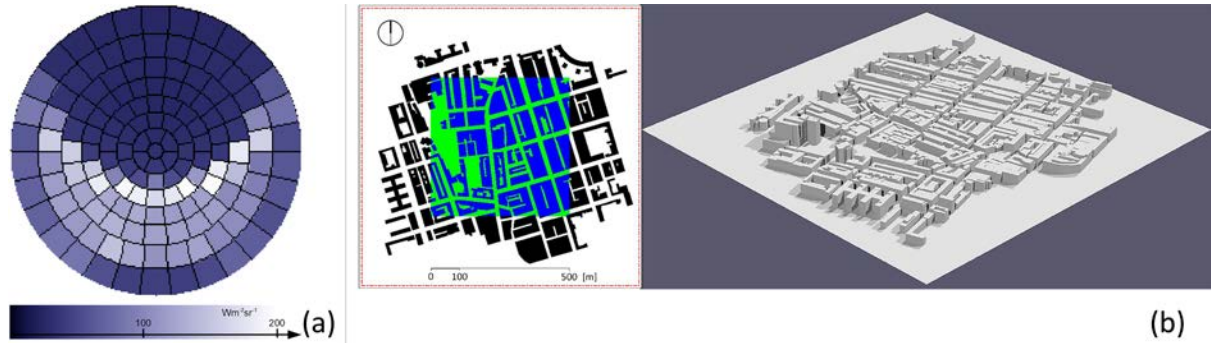
Figure 2: (a): Stereographic view of the sky vault representing London's annual sky model used for irradiance simulations. (b): Left, ground map of C2 urban form, in colour the simulated area and in black the surrounding buildings; right, its perspective view in PPF.

Results

Mean façade SVF and irradiances by urban form

Figure 3 illustrates annual mean irradiances and mean SVF values computed for each of the 24 urban forms, ranked (from left to right) in decreasing order of density. As implied by the line chart, the relationship between mean façade SVF and density is clearly negative with the coefficient of determination (R^2) being 0.92. The colour bars allow the comparison of the percentages in which annual global irradiance consists of direct, sky diffused and reflected irradiation. It is ascertained that, in all the urban forms, façades' annual global irradiance consists constantly of direct radiation by 42-43%, sky diffused by 44-45% and reflected by 13-14%. Hence, sky diffused radiation constitutes the greatest part of annual irradiation received by building façades in London, with direct solar contribution though being equally important.

The linear regression analysis revealed a particularly strong, positive correlation between SVF and all three irradiances comprising global irradiance (R^2>0.98) and so, not surprisingly, the relationship between SVF and global irradiance was found to be almost perfectly linear (R^2=0.99). It is pointed out that, since global irradiance expresses the sum of three irradiance components, its statistical relationship with SVF is determined by the relationship of each of its components with SVF, weighted by their percentages.
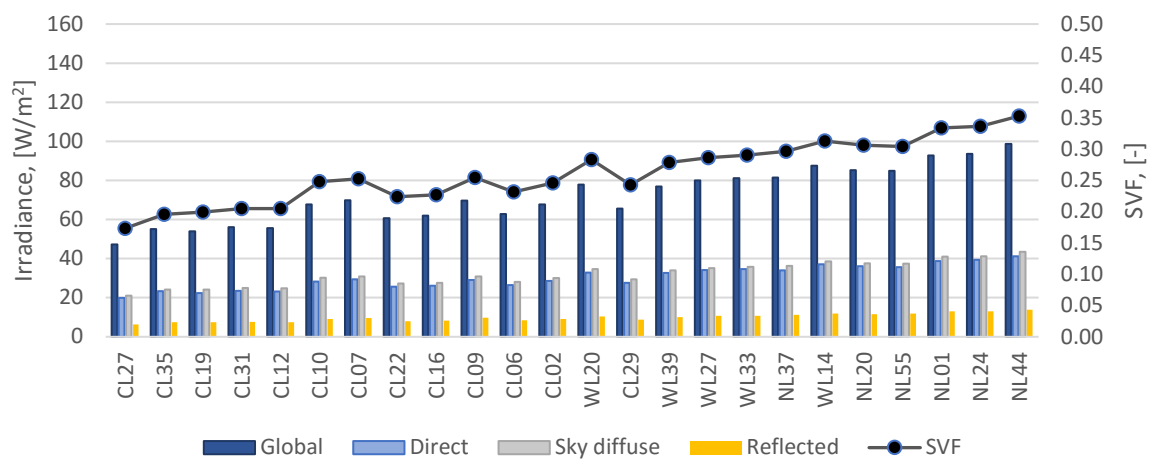

Figure 3. Mean façade SVF (dots, right vertical axis) and annual global, direct, sky diffused and reflected irradiance values (bars, left vertical axis) by urban form.

Mean façade SVF and irradiances by orientation

In the previous section, average façade SVF and irradiance values in the urban forms were found to correlate particularly highly, independently to type of irradiance. Nonetheless, solar availability on building façades and, especially the direct solar radiation received by them, is strongly affected by their orientation in relation to the sun path. Thus, the averaging of solar irradiance values over entire urban forms may suppress significant variations of the studied relationships occurring at different orientations. For this reason, the relationships between mean façade SVF and irradiances were also examined by orientation, considering 30 orientations at 12° azimuth intervals; these represent the patches into which the perimeter of the sky models is divided (see Fig. 2a). The numbering of the orientations starts from North (Orientation 1: -6 ≤ azimuth < 6) and counts clockwise.

Once mean SVF and irradiances were computed for all 30 orientations by urban form, the obtained values were classified by orientation. In total, 120 regression analysis tests, i.e. 30 orientations by four types of irradiance, were performed. For some orientations, the regression was based on less than 24 cases as some urban forms present very few points (<10) facing at specific orientations. In all cases though, the number of urban forms considered were not less than 20.
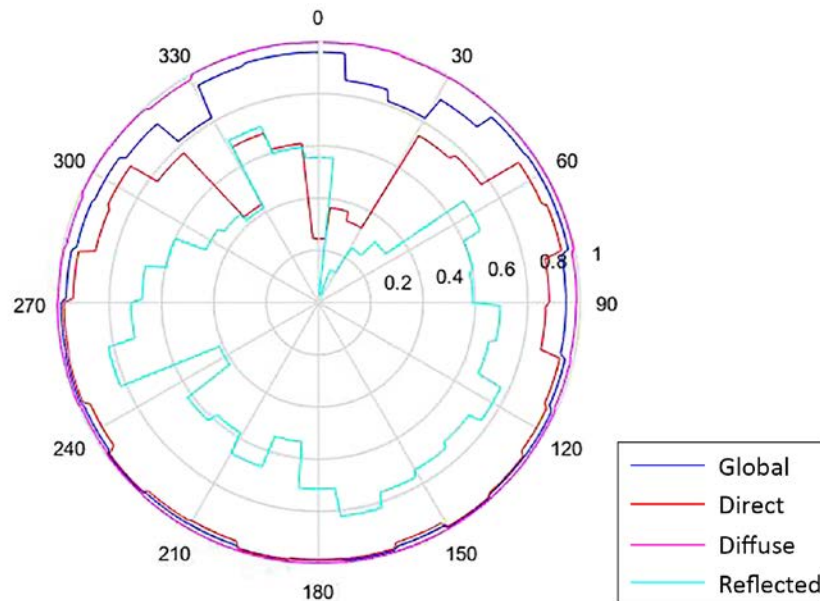

Figure 4. Variations of R^2 -measured from centre outwards- describing the linear relationship of SVF and annual mean irradiances, i.e. global, direct, diffuse, and reflected, by orientation.

The R^2 describing the strength of the relationship between mean SVF and annual irradiances are presented graphically in a polar chart in Figure 4, with the values being measured from the center outwards. As may be expected, the relationship between SVF and sky diffused irradiance is found to be almost perfectly linear for all orientations. Regarding direct irradiance though, the relationship is clearly affected by orientation: it is significantly strong (R^2>0.8) for façade azimuths between 60° and 300° (from East to West) whereas, for the remaining orientations, the R^2 values are reduced and vary unevenly. This may be partially attributed to low solar altitudes coinciding with north orientations (Chatzipoulka et al., 2015). On the other hand, the relationship between SVF and irradiance reflected by buildings appears to be independent to orientation as the R^2 fluctuates unevenly around different orientations. Finally, regarding global irradiance, it is of great interest that the R^2 value is

constantly above 0.8. This is explained by the following: (i) the reflected part comprises a small percentage of the total irradiance received by building façades, and (ii) the solar irradiation of façades facing to north orientations is dominated by sky diffused radiation.

Predicting annual global irradiance on façades in London

Since mean façade SVF presents an almost perfectly linear relationship with annual mean global irradiance, independently to orientation, it is argued that SVF can be used as a good predictor of solar energy potential of façades. This section provides a graphical tool to architects and urban designers based in London for estimating annual global irradiance on a façade, as a function of its azimuth angle and mean SVF. For this purpose, linear regression analysis was repeated setting intercept value to zero and 30 analytical models i.e. one for each orientation, were obtained; the beta coefficients (b) are presented in Table 1. As shown in Figure 5, which demonstrates the scatter plots and linear resolutions for six representative orientations, setting intercept to zero affects slightly the strength of the relationship with R^2 remaining significantly high.

The linear functions were next solved for 10 representative SVF values, from 0 to 0.5, at 0.05 intervals, and the (x, y) points are plotted on Cartesian axes as continuous curves. The relevant graph is presented in Figure 6; the suggested way of using it is as follows:

- identify the azimuth degree of the façade of interest on the horizontal axis;
- from that point, draw a normal line to intersect the curve representing SVF value closest to mean SVF of the façade;
- project the intersection point on the vertical axes to read the estimated annual mean global irradiance [W/m^2] (left) and solar irradiation [kWh/m^2] (right).
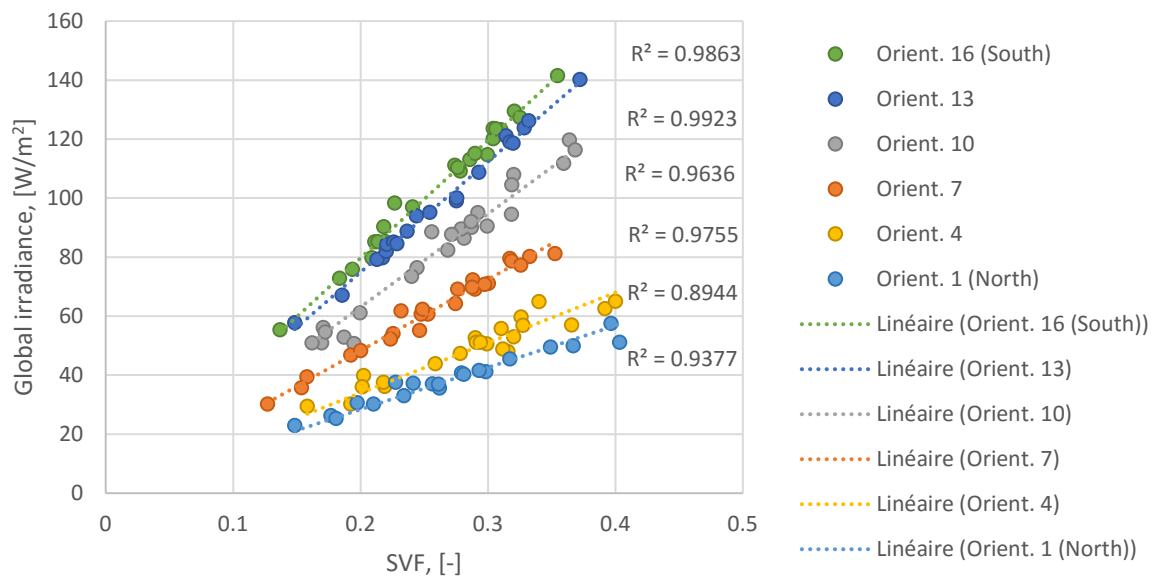

Figure 5. Mean global irradiance plotted against mean SVF values for six representative orientations, and their linear regression by setting intercept value to 0.

Table 1: Coefficients (b) for estimating annual global irradiance (Ig) as function of SVF for all different orientations, where Ig = b * SVF.

azimuth, a [°]	North: -6 ≤ a < 6	Orient. 2: 6 ≤ a < 18	Orient. 3: 18 ≤ a < 30	Orient. 4: 30 ≤ a <42	Orient. 5: 42 ≤ a < 54	Orient. 6: 54 ≤a <66	Orient. 7: 66 ≤ a < 78	Orient. 8: 78 ≤ a <90	Orient. 9: 90 ≤ a < 102	Orient. 10: 102≤a <114
b	141.95	143.54	150.96	169.94	190.93	215.41	241.5	264.72	291.80	315.55
azimuth, a [°]	Orient. 11: 114≤a <126	Orient. 12: 126≤a <138	Orient. 13: 138≤a <150	Orient. 14: 150≤a <162	Orient. 15: 162≤a <174	South: 174≤a <186	Orient. 17: 186≤a <198	Orient. 18: 198≤a <210	Orient. 19: 210≤a <222	Orient. 20: 222≤a <234
b	338.2	355.6	374.51	388.2	394.56	398.49	398.36	392.70	382.10	367.65
azimuth, a [°]	Orient. 21: 234≤a <246	Orient. 22: 246≤a <258	Orient. 23: 258≤a <270	Orient. 24: 270≤a <282	Orient. 25: 282≤a <294	Orient. 26: 294≤a <306	Orient. 27: 306≤a <318	Orient. 28: 318≤a <330	Orient. 29: 330≤a <342	Orient. 30: 342≤a <354
b	345.46	321.44	302.34	276.18	243.38	213.78	193.56	172.76	154.06	145.06

To test the validity of the prediction models, annual global irradiance was computed on the facades of a single, unobstructed building of triacontagonal plan (i.e. featuring 30 façades, pointing at the middle of orientation intervals). Comparing the results with values derived by solving the models for SVF equal to 0.5 - represented by the upper, light blue curve in Figure 6 -, it was found that the latter tend to slightly overestimate façades' annual global irradiance; however, there is still a very good agreement. Indicatively, the relative difference between values derived from the models and those simulated for the test is on average 3.7%, and the greatest differences, about 6.5%, are observed for façade orientations receiving annually more solar radiation, i.e. south orientations.
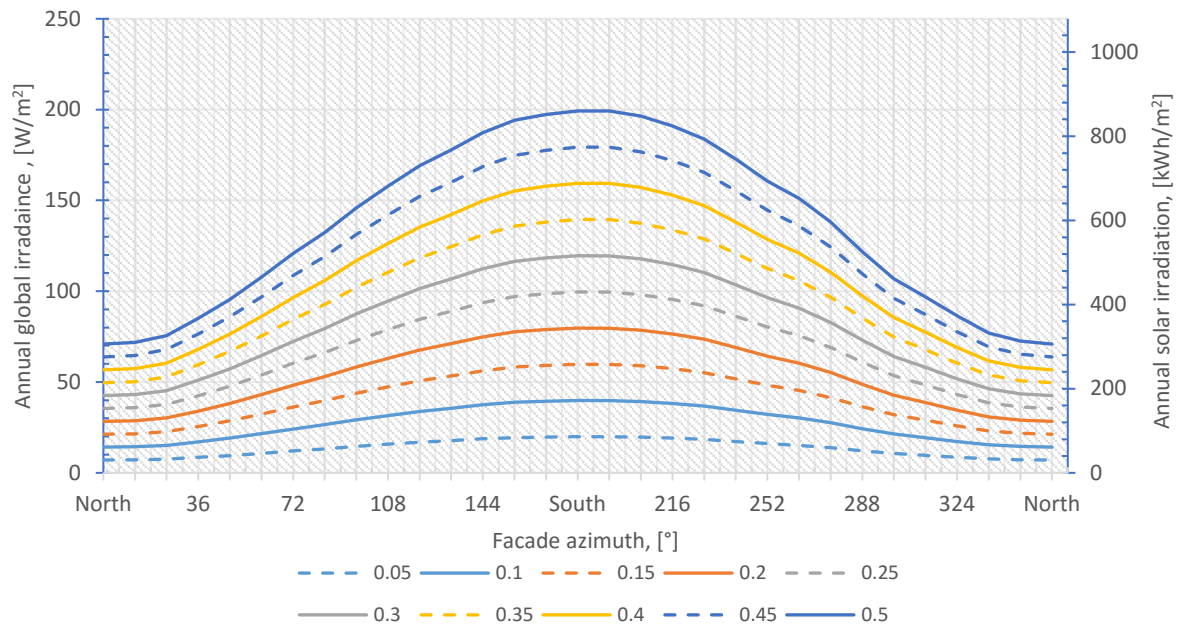

Figure 6. Graphical tool for estimating annual global irradiance on (left) and solar irradiation of (right) a vertical surface in London, as a function of its azimuth angle and mean SVF.

Conclusions and further research

Evaluating solar energy potential of façades using their SVF values would be of great relevance to professionals working in the field of urban environmental design. SVF is exclusively defined by urban geometry and thus its calculation is more straightforward compared to solar simulations. Using the case of London, the present study demonstrates that this is feasible since SVF was found to have a strong linear relationship with annual global irradiance, independently to façade orientation. To exemplify the usability of such a finding, the linear models obtained from regression analysis are integrated into a graphical tool for predicting annual solar irradiation of a façade surface, based on its SVF and azimuth angle.

Additionally, the fact that SVF was found to correlate well with both dominant components of solar irradiation, namely sky diffused radiation and direct radiation for major orientations (i.e. azimuths described by the annual sun path), indicates that SVF can be used as a predictor of annual solar availability at latitudes similar to London, even for sunnier climates. To test the sensitivity of the findings to other time periods and latitudes, the analysis has been extended to a winter month, January, and a summer month, July, considering two more European cities, Athens and Helsinki. Overall, the results confirm the strong relationship between SVF and solar irradiation of facades, and are reserved for a future publication.

Acknowledgements

References

Chatzipoulka, C., Nikolopoulou, M., Watkins, R. (2015). The impact of urban geometry on the radiant environment in outdoor spaces. In: *ICUC9 9th International Conference on Urban Climate*, Toulouse, France, 20-24 July 2015.

Chatzipoulka, C., Compagnon, R., Nikolopoulou, M. (2016). Urban geometry and solar availability on façades and ground of real urban forms: using London as case study. *Solar Energy*, 138, pp. 53-66.

Cheng, V., Steemers, K., Montavon, M., Compagnon, R. (2006). Compact cities in a sustainable manner. In: *2nd International Solar Cities Congress*, Oxford, UK, 3-6 April 2006.

Compagnon, R. (2004). Solar and daylight availability in the urban fabric. *Energy and Buildings,* 36(4), pp. 321–328.

Eliasson, I. (1996). Urban nocturnal temperatures, street geometry and land use. *Atmospheric Environment*, 30(3), pp. 179-192.

EPBD (2010). Directive 2010/31/EU of the European Parliament and of the Council of 19 May 2010 on the energy performance of buildings. *Official Journal of the European Union*, pp. 13-35.

Esclapés, J., Ferreiro, I., Piera, J., Teller, J. (2014). A method to evaluate the adaptability of photovoltaic energy on urban façades. *Solar Energy*, 105, pp. 4141-427.

International Energy Agency (2014). *World Energy Outlook*. Paris: OECD Publishing.

Mohajeri, N., Upadhyay, G., Gudmundsson, A., Assouline, D., Kämpf, J., Scartezzini, J.-L. (2016). Effects of urban compactness on solar energy potential. *Renewable Energy*, 93, pp. 469–482.

Project PREcis (2000). *PREcis: Assessing the Potential for Renewable Energy in Cities.* Final report, Project no. JOR3-CT97-0192, 2000.

Ratti, C., Raydan, D., Steemers, K. (2003). Building form and environmental performance: Archetypes, analysis and an arid climate. *Energy and Buildings*, 35(1), pp. 49-59.

Redweik, P., Catita, C., Brito, M. (2013). Solar energy potential on roofs and facades in an urban landscape. *Solar Energy*, 97, pp. 332-341.

Remund, J., Müller, S., Kunz, S., Huguenin-Landl, B., Studer, C., Klauser, D., Schilter, C., Lehnherr, R. (2015). *METEONORM – Global Meteorological Database*, Handbook Part I & II, Version 7. Bern: Meteotest & Swiss Federal Office for Energy.

Ward Larson, G., Shakespeare, R. (1998). *Rendering with Radiance: The Art and Science of Lighting Visualisation*. San Francisco: Morgan Haufmann.

Yamashita, S., Sekine K., Shoda M., Yamashita, K., Hara, Y. (1986). On relationships between heat island and sky view factor in the cities of Tama River basin, Japan. *Atmospheric Environment*, 20(4), pp. 681-686.

Yun, G.Y., Steemers, K. (2009). Implications of urban settings for the design of photovoltaic and conventional façades. *Solar Energy*, 83, pp. 69-80.

Zhang, J., Heng, C.K., Malone-Lee, L.C., Hii, D.J.C., Janssen, P., Leung, K.S., Tan, B.K. (2012). Evaluating environmental implications of density: A comparative case study on the relationship between density, urban block typology and sky exposure. *Automation in Construction*, 22, pp. 90-101.